Long-Range Exchange Interactions and Integer-Spin $S_t = 2$ EPR Spectra of a $Cr^{III}Zn^{II}Cr^{III}$ Species with Multiplet Mixing

Dirk Burdinski, Eckhard Bill,* Frank Birkelbach, Karl Wieghardt, and Phalguni Chaudhuri*

Max-Planck-Institut für Strahlenchemie, Stiftstrasse 34-36, D-45470 Mülheim an der Ruhr, Germany

Received August 1, 2000

Synthesis, structural, and spectroscopic characterization of the linear cationic complex $[LCr^{III}\{\mu\text{-}[dmg)_3Zn^{II}\}\text{-}Cr^{III}L]^{2+}$ (**1**) in which L = 1,4,7-trimethyl-1,4,7-triazacyclononane and dmg is the dimethylglyoximato anion are reported. The Cr···Cr distance of **1** is 7 Å. SQUID magnetic susceptibility measurements reveal the presence of long-range exchange interaction of the Cr^{III} terminal ions, mediated by the diamagnetic $Zn^{II}(dmg)_3$ "bridging ligand" ($J_0 = -4.4$ cm^{-1}, $H_{ex} = -2J_0S_1S_2$, $S_i = {}^3/_2$). Multifrequency EPR measurements (S-, X-, Q-band) on frozen solutions were used to establish the *intramolecular* nature of the exchange coupling and to determine the zero-field splitting (ZFS) parameters and the anisotropic contributions of spin coupling. An effective spin Hamiltonian description was applied for interpretation of the spectra originating from the $S_t = 2$ total spin manifold which included up to fourth-order terms for the ZFS. By the help of alternative simulations with the full coupling matrix for two spins $S_i = {}^3/_2$ (16 × 16) it could be shown that the higher-order terms in the effective description owe their origin to multiplet mixing due to competing single-ion ZFS ($|D_i| = 0.2$ cm^{-1}) and isotropic exchange interaction. The magnetic anisotropy related to dimer properties could be readily explained by dipolar coupling ($j_z = -0.012$ cm^{-1}). Implications for the interpretation of other integer-spin EPR spectra are discussed.

Introduction

This work forms a part of our program on exchange interactions[1−4] in linear trinuclear complexes and deals specifically with the case of the $d^3d^{10}d^3$ electronic configuration, for which studies related to long-range exchange interactions are rare.[5] Herein we explore the effects of increasing the charge of the terminal paramagnetic centers, viz., Cr(III), from +3 to +4 (viz., in Mn(IV)) on the strength of the exchange interactions. The above objective has been realized by synthesizing isostructural and isoelectronic linear complexes $Cr^{III}Zn^{II}Cr^{III}$ and $Mn^{IV}Zn^{II}Mn^{IV}$ containing three dioximato anions as bridging ligands. We report here the synthesis, magnetic, and spectroscopic (EPR) properties together with the X-ray structural characterization of $[LCr^{III}\{\mu\text{-}(dmg)_3Zn^{II}\}Cr^{III}L](ClO_4)_2$, **1**, and compare the properties of **1** with those of its congeners $[LMn^{IV}\{\mu\text{-}(dmg)_3Zn^{II}\}Mn^{IV}L](ClO_4)_4$, **2**, where L represents the tridentate amine ligand 1,4,7-trimethyl-1,4,7-triazacyclononane and dmg is the dimethylglyoximato dianion. Similar dioximato-bridged trinuclear complexes of general formula have been described earlier by us.[6−8] (See Chart 1.)

Chart 1

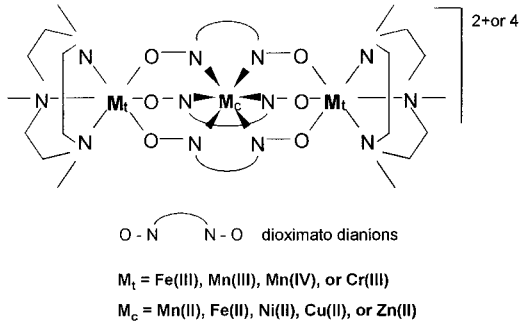

Experimental Section

Chemicals. The macrocycle 1,4,7-trimethyl-1,4,7-triazacyclononane ($L = C_9H_{21}N_3$) and its chromium(III) complex $LCrBr_3$ were prepared as described previously.[9,10] All other starting materials were commercially available and mostly of reagent grade. Elemental analyses (C, H, N) were performed by the Microanalytical Laboratory, Ruhr-Universität Bochum. Chromium was determined spectrophotometrically as chromate at $\lambda = 370$ nm ($\epsilon = 4960$ l mol^{-1} cm^{-1}). Zinc was determined by AAS. The perchlorate anion was determined gravimetrically as tetraphenylarsonium perchlorate.

Physical Measurements. Fourier transform infrared spectroscopy on KBr pellets was performed on a Perkin-Elmer 1720X FT-IR instrument. Electronic absorption spectra were measured on a Perkin-Elmer Lambda 9 spectrophotometer in solution. Magnetic susceptibili-

* Authors to whom correspondence should be addressed. E-mail: bill@mpi-muelheim.mpg.de; chaudh@mpi-muelheim.mpg.de.

(1) Birkelbach, F.; Winter, M.; Flörke, U.; Haupt, H.-J.; Butzlaff, C.; Lengen, M.; Bill, E.; Trautwein, A. X.; Wieghardt, K.; Chaudhuri, P. *Inorg. Chem.* **1994**, *33*, 3990.
(2) Chaudhuri, P.; Winter, M.; Della Védova, B. P. C.; Fleischhauer, P.; Haase, W.; Flörke, U.; Haupt, H.-J. *Inorg. Chem.* **1991**, *30*, 4777.
(3) Chaudhuri, P.; Birkelbach, F.; Winter, M.; Staemmler, V.; Fleischhauer, P.; Haase, W.; Flörke, U.; Haupt, H.-J. *J. Chem. Soc., Dalton Trans.* **1994**, 2313.
(4) Birkelbach, F.; Weyhermüller, T.; Lengen, M.; Gerdan, M.; Trautwein, A. X.; Wieghardt, K.; Chaudhuri, P. *J. Chem. Soc., Dalton Trans*, **1997**, 4529.
(5) Corbin, K. M.; Gleurup, J.; Hodgson, D. J.; Lynn, M. H.; Michelsen, K.; Nielsen, K. M. *Inorg. Chem.* **1993**, *32*, 18.
(6) Chaudhuri, P.; Winter, M.; Fleischhauer, P.; Haase, W.; Flörke, U.; Haupt, H.-J. *J. Chem. Soc., Chem. Commun.* **1990**, 1728.
(7) Birkelbach, F.; Flörke, U.; Haupt, H.-J.; Butzlaff, C.; Trautwein, A. X.; Wieghardt, K.; Chaudhuri, P. *Inorg. Chem.* **1998**, *37*, 2000.
(8) Burdinski, D.; Birkelbach, F.; Weyhermüller, T.; Flörke, U.; Haupt, H.-J.; Lengen, M.; Trautwein, A. X.; Bill, E.; Wieghardt, K.; Chaudhuri, P. *Inorg. Chem.* **1998**, *37*, 1009.
(9) Chaudhuri, P.; Winter, M.; Küppers, H.-J.; Wieghardt, K.; Nuber, B.; Weiss, J. *Inorg. Chem.* **1987**, *26*, 3302.
(10) Wieghardt, K.; Chaudhuri, P.; Nuber, B.; Weiss, J. *Inorg. Chem.* **1982**, *21*, 3086.

10.1021/ic000870h CCC: $20.00
Published on Web 02/10/2001

Table 1. Crystallographic Data for $[L_2Cr^{III}_2(dmg)_3Zn^{II}](ClO_4)_2 \cdot CH_3OH$, **1**

chem formula	$C_{31}H_{64}N_{12}O_{15}Cl_2Cr_2Zn$	ρ_{calc}, g cm^{-3}	1.587
fw	1085.20	diffractometer	Siemens P4
cryst size, mm	0.55 × 0.30 × 0.20	λ(Mo Kα), Å	0.71073
cryst syst	monoclinic	μ, mm^{-1}	1.188
space group	*C*2/*c*	no. of indep refltns ($F > 4.0\sigma(F)$)	2325
a, Å	28.94(2)		
b, Å	12.040(10)		
c, Å	14.845(11)	R_F [a] ($F > 4\sigma(F)$)	0.056
V, Å^3	4543(6)	*T*, K	193(2)
Z	4		

[a] $R_F = \sum(|F_o| - |F_c|)/\sum|F_o|$.

ties of powdered samples were recorded on a SQUID magnetometer (MPMS, Quantum Design) in the temperature range 2−295 K with an applied field of 1 T. Experimental susceptibility data were corrected for the underlying diamagnetism by using Pascal's constants. The magnetic data were simulated by using the spin-Hamiltonian program JULIUS.[11] X-band EPR spectra were recorded either of the polycrystalline material or on solutions at various temperatures between 3 and 100 K with a Bruker ESP 300E spectrometer equipped with a standard TE 102 cavity, an Oxford Instruments liquid helium continuous-flow cryostat, a NMR gaussmeter, and a frequency meter. Spin-Hamiltonian simulations of integer-spin ($S = 2$) and coupled-spin EPR spectra were achieved with our own computer programs which were developed from the routine published[12] by B. Gaffney and J. Silverstone for $S = {}^5/_2$. The programs perform full-matrix diagonalization, and powder spectra were summed up in an octant of the unit sphere on a rectangular (θ, Ψ) mesh with 90 × 90 points. The routines are accomplished with a SIMPLEX fitting shell[13] for parameter optimization. Error ranges were estimated by systematic detuning of the individual parameters and evaluation of the obtained results by comparison with the optimized spectra.

Preparation of Complexes. $[LCr^{III}\{\mu\text{-}(dmg)_3Zn^{II}\}Cr^{III}L](ClO_4)_2 \cdot CH_3OH$, 1. A suspension of $LCrBr_3$ (0.93 g, 2.0 mmol), dimethylglyoxime (0.35 g, 3.0 mmol), $Zn(ClO_4)_2 \cdot 6H_2O$ (0.37 g, 1 mmol), and triethylamine (2.0 mL, 14 mmol) in methanol (80 mL) was refluxed for 12−15 h. The reaction was complete when there was no solid present and a clear deep red solution was obtained. The hot solution was eventually filtered to remove any solid particle, and a solution of $NaClO_4 \cdot H_2O$ (2.0 g, 14 mmol) in methanol was added to it. The solution yielded after 2−3 days red-brown crystals of **1**, which lost CH_3OH on exposure to air. The substance can be recrystallized from methanol. Yield: 0.63 g (58%). Anal. Calcd for $C_{30}H_{60}N_{12}O_6Cr_2Zn(ClO_4)_2 \cdot CH_3OH$: C, 34.31; H, 5.94; N, 15.49; Cr, 9.58; Zn, 6.02; ClO_4, 18.32. Found: C, 34.6; H, 6.0; N, 15.4; Cr, 9.4; Zn, 6.0; ClO_4, 18.2. IR (KBr, cm^{-1}): ν(NO) 1186m, ν(CN) 1599m. UV−vis in CH_3CN: λ_{max}, nm (ϵ, M^{-1} cm^{-1}): 273 (32000), 425 (740), 526 (236). MS (*m*/*z*): 989.2, 873.2.

$[LMn^{IV}\{\mu\text{-}(dmg)_3Zn^{II}\}Mn^{IV}L](ClO_4)_4$, 2. The compound has been prepared as described earlier.[7]

CAUTION! Although we experienced no difficulties, the unpredictable behavior of perchlorate salts necessitates extreme caution in their handling.

X-ray Structure Determination. X-ray diffraction data for a red-brown crystal of complex **1** were collected at 193 K with a Siemens P4 diffractometer using graphite-monochromatized Mo Kα radiation ($\lambda = 0.71073$ Å). A summary of the crystallographic data and structure refinement parameters for **1** is given in Table 1. Data were collected by the $2\theta/\omega$-scan method for **1** ($3° \le 2\theta \le 50°$). Three standard reflections monitored every 100 reflections showed no significant variations. The data were corrected for absorption[14] and Lorentz−polarization effects. The structure was solved by conventional Patterson and difference Fourier methods by using the Siemens SHELXTL-PLUS package.[15] The function minimized during full-matrix least-squares refinement was $\sum\omega(|F_o| - |F_c|)^2$, where $\omega^{-1} = \sigma^2(F) = +0.0007F^2$. Neutral atom scattering factors and anomalous dispersion corrections for non-hydrogen atoms were taken from ref 16. The hydrogen atoms were placed at calculated positions with isotropic thermal parameters; the methyl groups were treated as rigid bodies. All non-hydrogen atoms were refined with anisotropic thermal parameters.

Chart 2

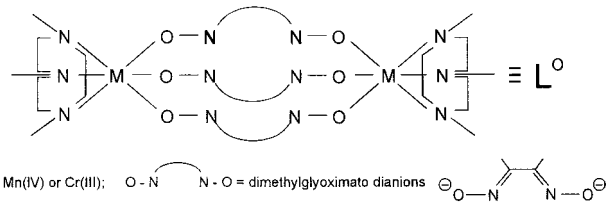

Results and Discussion

A straightforward synthetic route to the pure heterotrinuclear complex $Cr^{III}Zn^{II}Cr^{III}$, **1**, containing tris(dimethylglyoximato) bridges has been developed which affords large quantities of pure crystalline product in more than 50% yield. The kinetic inertness of trivalent chromium ion resulting from a d^3 electron configuration and the lability of the divalent metal ions like Zn(II) are utilized to synthesize $Cr^{III}Zn^{II}Cr^{III}$ trinuclear complex. Practically no scrambling was observed, probably because the reaction temperature was too low to surmount the activation barrier to dissociation. In contrast to other synthetic routes known for mixed-metal complexes,[17] it was not necessary to isolate the intermediate $Zn(dmg)_3^{4-}$ for this synthetic route. **1** was prepared directly by refluxing a suspension of $LCrBr_3$ and dimethylglyoxime with the right stoichiometry in the presence of triethylamine to which Zn(II) was added. It is conceivable that the central zinc metal ion acts as a template center for the formation of the bicyclic ring present in **1**. The concept of a template synthesis as a mechanism for the macrobicycle formation has been proposed for the similar B(III)-capped clathrochelates.[18,19] The preparation of the isoelectronic species $[L_2Mn^{IV}_2Zn^{II}(dmg)_3](ClO_4)_4$, **2**, has been described earlier.[7,20] Its cyclohexane-1,2-dionedioxime (nioxime), i.e., analogue $[L_2Mn^{IV}_2Zn^{II}(niox)_3](ClO_4)_4$, has also been structurally characterized.[4] Compounds **1** and **2** may be considered as coordination complexes containing an ion, Zn^{2+}, totally encapsulated by a metallabicyclic ligand L^o, shown in Chart 2. A similar example of a clathrochelate, $[(dien)_2Cr^{III}_2(dmg)_3Co^{III}]^{3+}$, with diethylenetriamine(dien) as the capping-amine ligand, has been reported[21] but was not structurally characterized.

(11) Krebs, C.; Birkelbach, F.; Staemmler, V. Unpublished
(12) Gaffney, B. J.; Silverstone, H. J. Simulation of the EMR Spectra of High-Spin Iron in Proteins. In *Biological Magnetic Resonance*; Berliner, L. J., Reuben, J., Eds.; Plenum Press: New York, London, 1993; Vol. 13.
(13) Press, W. H.; Flannery, B. P.; Teukolsky, S. A.; Vetterling, W. T. *Numerical Recipes*; Cambridge University Press: Cambridge, 1990.
(14) Walker, N. *Acta Crystallogr.* **1983**, *A39*, 158.
(15) SHELXTL-PLUS program package (PC version of G. M. Sheldrick, Universität Göttingen, 1990).
(16) *International Tables for X-ray Crystallography*; Kynoch: Birmingham, England, 1974; Vol. 4.
(17) See, for example: Kahn, O. *Struct. Bonding (Berlin)* **1987**, *68*, 89.
(18) (a) Boston, D. R.; Rose, N. J. *J. Am. Chem. Soc.* **1968**, *90*, 6859. (b) Boston, D. R.; Rose, N. J. *J. Am. Chem. Soc.* **1973**, *95*, 4163. (c) Jackels, S. C.; Rose, N. J. *Inorg. Chem.* **1973**, *12*, 1232.
(19) (a) Parks, J. E.; Wagner, B. E.; Holm, R. H. *J. Am. Chem. Soc.* **1970**, *92*, 3500. (b) Larsen, E.; La Mar, G. N.; Wagner, B. E.; Parks, J. E.; Holm, R. H. *Inorg. Chem.* **1972**, *11*, 2652. (c) Rai, H. C.; Jena, A. K.; Sahoo, B. *Inorg. Chim. Acta* **1979**, *35*, 29. (d) Voloshin, Y. Z.; Kostromina, N. A.; Nazarenko, A. Y. *Inorg. Chim. Acta* **1990**, *170*, 181. (e) Voloshin, Y. Z.; Belsky, V. K.; Trachevskii, V. V. *Polyhedron* **1992**, *11*, 1939. (f) Kubow, S. A.; Takeuchi, K. J.; Grzybowski, J. J.; Jircitano, A. J.; Goedken, V. L. *Inorg. Chim. Acta* **1996**, *241*, 21. (g) Robbins, M. K.; Naser, D. W.; Heiland, J. L.; Grzybowski, J. J. *Inorg. Chem.* **1985**, *24*, 3381.
(20) Chaudhuri, P.; Winter, M.; Birkelbach, F.; Fleischhauer, P.; Haase, W.; Flörke, U.; Haupt, H.-J. *Inorg. Chem.* **1991**, *30*, 4291.

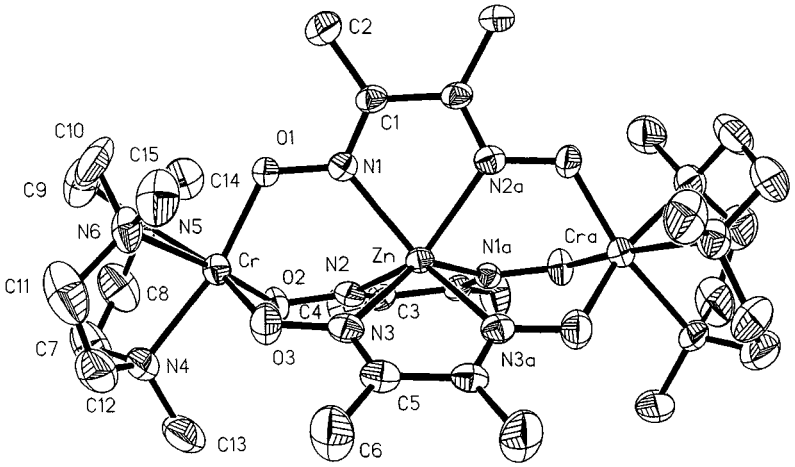

Figure 1. Molecular structure of **1**.

Discussion of the IR absorptions is confined to the most important vibrations of the 4000−400 cm^{-1} region in relation to the structure. **1** exhibits a strong band at 1097 cm^{-1} (antisymmetric stretch) and a sharp band at 625 cm^{-1} (antisymmetric bend), indicative of uncoordinted perchlorate anions. The ν(CN) vibration is assigned to the medium strong band at 1599 cm^{-1}. The band of medium strength at 1186 cm^{-1} is assignable to the NO stretching vibration in **1**. The second NO infrared absorption could not be observed because of the superposition of the strong band originating from the perchlorate anion. The corresponding IR absorptions for **2** have been described earlier.[7]

The optical spectrum of **1** has been measured in the range 200−1400 nm in dry acetonitrile to avoid any hydrolysis. The absorption maximum of the free oxime H_2dmg at 224 nm is due to $\pi-\pi^*$ transitions of the C═N groups and shifts to 265 nm in basic medium due to deprotonation of the OH groups. Similar $\pi-\pi^*$ transitions of the C═N groups are observed in **1**, as is evidenced by the band at 273 nm with an extinction coefficient of 3.2×10^4 M^{-1} cm^{-1}. The bands at 425 nm (ϵ = 740 M^{-1} cm^{-1}) and at 526 nm (ϵ = 236 M^{-1} cm^{-1}) are assigned to the spin-allowed transitions $^4A_2 \rightarrow {}^4T_1$ and $^4A_2 \rightarrow {}^4T_2$, respectively. It must be noted, as the d−d transitions of the formula 1, 2, 3 CrX_3Y_3 do not split appreciably in the trigonal (C_{3v}) ligand field and the energy of the first transition is equal to $10D_{q/av}$ ($=5D_{q/X} + 5D_{q/Y}$),[22,23] the band assignments have been performed similar to octahedral ligand field. It allows us to approximate the splitting parameter $10D_q \approx 19011$ cm^{-1}, which lie between those of the pure $Cr^{III}O_6$ and $Cr^{III}N_6$ chromophores. Similar ligand field parameters have been reported for, e.g., [1,2,3-Cr(dien)$(OH_2)_3]^{3+}$ (19600 cm^{-1}),[24] containing the mentioned CrN_3O_3 chromophore.

Molecular Structure of $[L_2Cr^{III}_2(dmg)_3Zn^{II}](ClO_4)_2\cdot CH_3OH$, 1. The molecular geometry and the atom-labeling scheme of the cation in **1** are shown in Figure 1. The structure of the complex cation consists of a discrete dicationic trinuclear centrosymmetric unit having a crystallographic 2-fold symmetry, two noncoordinatively bound perchlorate anions, and a molecule of solvent methanol. Selected bond lengths and angles are presented in Table 2. The X-ray structure confirms that a linear trinuclear complex, Cr−Zn−Cr(a) = 179.7(2)°, has indeed been formed in such a way that a tri-pseudooctahedral geometry containing a Zn(II) and two Cr(III) as central ions is present in the lattice. The central tris(dimethylglyoximato)zinc(II) ion, $[Zn(dmg)_3]^{4-}$, bridges two terminal chromium(III) centers through the deprotonated oxime oxygens. The central ZnN_6 core is nearly trigonal prismatic. The six oxime nitrogen atoms were arranged around the Zn(II) center with twist angles of 6.1°, 7.4°, and 7.4° between the triangular faces comprising N(1)N(2)N(3) and N(1a)N(2a)N(3a) atoms. In other words the coordination polyhedron is ca. 53° distorted from the ideal octahedral symmetry with a twist angle of 60°. The nearest neighbor Cr···Zn distance within the trinuclear cation is 3.570(3) Å. The nearest *intermolecular* Cr···Cr and Cr···Zn separations are 7.140 and 7.016 Å, respectively. The Zn−N(2) distance of 2.178(7) Å is slightly longer than the other two Zn−N(1) and Zn−N(3) bond lengths of 2.131(5) and 2.138(7) Å, respectively, and these distances are similar to those of the related $[L_2Mn^{III}_2(dmg)_3Zn]^{2+}$ cation.[20]

Table 2. Selected Bond Lengths (Å) and Angles (deg) for $[L_2Cr^{III}_2(dmg)_3Zn](ClO_4)_2\cdot CH_3OH$, **1**

	Cr−Zn−Cr(a)	179.7(2)	
Cr···Zn	3.570(3)	Cr···Cr(a)	7.140(4)
Zn−N(1)	2.131(5)	Zn−N(2)	2.178(7)
Zn−N(3)	2.138(7)		
Cr−N(4)	2.129(8)	Cr−N(5)	2.123(8)
Cr−N(6)	2.126(6)	Cr−O(1)	1.922(6)
Cr−O(2)	1.936(4)	Cr−O(3)	1.911(6)
N(1)−O(1)	1.360(9)	N(1)−C(1)	1.282(10)
N(2)−O(2)	1.364(9)	N(2)−C(3)	1.264(8)
N(3)−O(3)	1.348(9)	N(3)−C(5)	1.257(10)
N(1)−Zn−N(2)	85.9(2)	N(1)−Zn−N(3)	89.1(2)
N(2)−Zn−N(3)	88.2(2)	N(1)−Zn−N(1A)	124.4(3)
N(1)−Zn−N(2A)	73.8(2)	N(2)−Zn−N(2A)	135.7(3)
N(3)−Zn−N(2A)	129.2(2)		
N(1)−Zn−N(3A)	139.4(2)		
N(3)−Zn−N(3A)	74.4(4)		
		N(4)−Cr−N(5)	82.1(3)
N(4)−Cr−N(6)	82.2(3)	N(5)−Cr−N(6)	82.0(3)
N(4)−Cr−O(1)	168.4(2)	N(5)−Cr−O(1)	90.0(3)
N(6)−Cr−O(1)	88.3(2)	N(4)−Cr−O(2)	91.2(2)
N(5)−Cr−O(2)	88.9(2)	N(6)−Cr−O(2)	169.3(3)
O(1)−Cr−O(2)	97.2(2)	N(4)−Cr−O(3)	87.6(3)
N(5)−Cr−O(3)	166.9(3)	N(6)−Cr−O(3)	88.6(2)
O(1)−Cr−O(3)	98.9(3)	O(2)−Cr−O(3)	99.5(2)
Zn−N(1)−O(1)	124.7(4)	Zn−N(1)−C(1)	117.8(5)
O(1)−N81)−C(1)	117.2(5)	Zn−N(2)−O(2)	124.6(4)
Zn−N(2)−C(3)	116.6(6)	O(2)−N(2)−C(3)	118.5(7)
Zn−N83)−O(3)	125.1(5)	Zn−N(3)−C(5)	117.0(6)
O(3)−N(3)−C(5)	117.8(7)		

(21) Drago, R. S.; Elias, J. H. *J. Am. Chem. Soc.* **1977**, *99*, 6570.
(22) Krishnamurthy, R.; Schapp, W. *J. Chem. Educ.* **1969**, *46*, 799.
(23) Lever, A. B. P. *Inorganic Electronic Spectroscopy*, 2nd ed.; Elsevier: New York, 1984.
(24) Caldwell, S. H.; House, D. A. *J. Inorg. Nucl. Chem.* **1969**, *31*, 811.

The coordination geometry of the terminal chromium ion is distorted octahedral with three nitrogen atoms N(4), N(5), and N(6) from the facially coordinated tridentate macrocyclic amine (L) and three oxygen atoms, O(1), O(2), and O(3), from three deprotonated dimethylglyoximato ligands, resulting in *fac*-CrN_3O_3 chromophores. The Cr−N (average 2.126(7) Å) and Cr−O (average 1.923(5) Å) distances are comparable to literature[9,25] values for chromium(III) complexes with this macrocyclic amine. The largest deviation from the idealized 90° interbond angles is 8°, which occurs within the five-membered C−C−N−Cr−N chelate rings, the N−Cr−N angles being average 82.1(1)°, whereas the O−Cr−O angles fall between 97.2(2)° and 99.5(2)°. An *intramolecular* Cr···Cr separation of 7.140(4) Å has been found.

The N−O (average 1.357(9) Å) and C═N (average 1.268(9) Å) bond lengths and the C−N−O bond angle (average 117.8-(6)°) of the bridging dimethylglyoximato ligands are found to be in good agreement with the previous studies.[26]

Magnetic and Electronic Properties. The paramagnetic properties of **1**, $Cr^{III}Zn^{II}Cr^{III}$, were analyzed by using the spin Hamiltonian for two coupled spins $S_i = {}^3/_2$ of the Cr^{III} pair with axial and rhombic single-ion zero-field splitting (ZFS) and anisotropic Zeeman interaction:

$$H = -2\mathbf{S}_1\cdot\tilde{\mathbf{J}}\cdot\mathbf{S}_2 + \sum_{i=1,2} D_i[S_{z,i}^2 - {}^{15}/_{12} + E/D_i(S_{x,i}^2 - S_{y,i}^2)] + \mu_B\mathbf{S}_i\cdot\tilde{\mathbf{g}}_i\cdot\mathbf{B} \quad (1)$$

The tensor $\tilde{\mathbf{J}} = J_0\,\tilde{\mathbf{1}} + \tilde{\mathbf{j}}$ in the Heisenberg−Dirac−van Vleck term describes the isotropic exchange (J_0) and the anisotropic ($\tilde{\mathbf{j}}$) exchange and dipolar interactions (if antisymmetric interaction is neglected[27]), D_i and E/D_i parametrize the axial and rhombic ZFS contributions, and $\tilde{\mathbf{g}}_i$ is the electronic $\tilde{\mathbf{g}}$ tensor of the Zeeman interaction.

In the limiting case of dominating isotropic exchange interaction ($|J_0| \gg D_i$) each of the isolated integer-spin manifolds $S_t = 1, 2, 3$ of the coupled system can be described by an effective spin Hamiltonian

$$H_t = D_t[S_{t,z}^2 - {}^1/_3S(S+1) + E/D_t(S_{t,x}^2 - S_{t,y}^2)] + O4_t + \mu_B\mathbf{S}_t\cdot\tilde{\mathbf{g}}_t\cdot\mathbf{B} \quad (2)$$

with different effective ZFS parameters D_t, E/D_t and $\tilde{\mathbf{g}}_t$ values for each state $S_t = 1, 2, 3$. The $O4_t$ term represents possible ZFS contributions of higher order (4th) in S_t which are usually neglected.[28,29] Distinct features of the experimental EPR spectra of **1** led us to introduce a symmetry-adapted fourth-order term in the effective spin Hamiltonian for $S_t = 2$:

$$O4_t = -{}^2/_3B_4\{O_4^0 + 20\sqrt{2}\,O_3^4\} + B_4^0\,O_4^0 \quad (3)$$

where the O_n^m represent equivalent operators[30] of fourth degree in S_t and the parameters B_4 and B_4^0 parametrize the cubic and trigonal fourth-order contributions to the ZFS.

(25) Chaudhuri, P.; Wieghardt, K. *Prog. Inorg. Chem.* **1987**, *35*, 329.
(26) See, for example: Morehouse, S. M.; Polychronopoulou, A.; Williams, G. J. B. *Inorg. Chem.* **1980**, *19*, 3558.
(27) Bencini, A.; Gatteschi, D. *EPR of Exchange Coupled Systems*; Springer: Berlin, New York, 1990.
(28) Mabbs, F. E.; Collison, D. *Electron Paramagnetic Resonance of d Transition Metal Compounds*; Elsevier: Amsterdam, 1992.
(29) Pilbrow, J. R. *Transition Ion Electron Paramagnetic Resonance*; Clarendon Press: Oxford, 1990.
(30) Abragam, A.; Bleaney, B. *Electron Paramagnetic Resonance of Transition Ions*; Oxford University Press: Oxford, 1970.

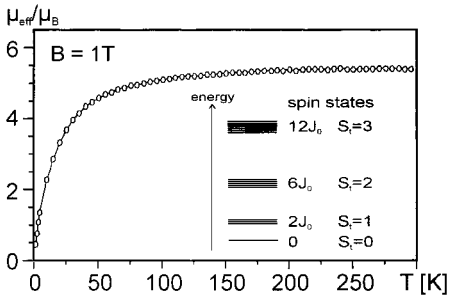

Figure 2. Temperature dependence of the effective magnetic moment of solid **1** measured at $B = 1$ T. The solid line is a fit by using eq 1 without ZFS and $\langle g_i\rangle = 2.03$, $J_0 = -4.4$ cm^{-1}. The fit contains contributions of an $S = {}^3/_2$ impurity species of 1.3%, based on the same molecular mass.

Magnetic susceptibility data of complex **1** were measured on polycrystalline samples in the temperature range 2−295 K with an applied field of 1 T (Figure 2). The temperature dependence of the effective magnetic moment $\mu_{eff}(T)$ shows a monotonic decrease from 5.47 μ_B at 295 K to 0.46 μ_B at 2 K, which is typical of an antiferromagnetically coupled two-spin system with total spin ground state $S_t = 0$. The magnetic data could be simulated by using an isotropic $\tilde{\mathbf{J}}$ tensor ($\tilde{\mathbf{J}} = J_0\,\tilde{\mathbf{1}}$); anisotropic exchange and dipolar contributions usually cannot be determined from powder measurements. Furthermore, also the ZFS parameters could not be derived from the static magnetic data of **1**, because in first order the nonmagnetic ground state is not affected by ZFS and the effects in the excited states are superimposed by dominating exchange splittings. Only from the EPR measurements (given below) in conjunction with the susceptibility result could reliable values for D_i and E/D_i be obtained. Temperature-independent paramagnetism (TIP) was not detected in the magnetic measurements; however, a monomeric impurity had to be considered to account for the residual magnetic moment of the solid sample at 2 K (1.3%, $S = {}^3/_2$). Fitting of the isotropic exchange and Zeeman terms yielded a value of the exchange coupling constant of $J_0 = -4.4$ cm^{-1}. This indicates the presence of appreciable spin coupling between the terminal metal ions Cr^{III}, separated by a large distance of ca. 7 Å.

EPR. In crystalline compound **1** the *intermolecular* separation of Cr^{III} ions in adjacent molecules is almost identical with the *intramolecular* Cr···Cr distance (∼7 Å). Therefore it could not be readily excluded that the observed antiferromagnetic spin coupling is due to *intermolecular* interactions in the solid. To rule out this possibility, temperature-dependent EPR measurements were performed on dissolved **1** in CH_3CN/DMF (1:3). At liquid helium temperatures well-resolved X-band spectra could be obtained which differ completely from what is expected for monomeric or weakly coupled Cr^{III} centers.[28,29] The derivative spectrum (Figure 3A) consists of six symmetrically split lines around $g = 2$ and a weak half-field signal close to $g = 4$. The pattern is typical of a spin manifold with high multiplicity and weak ZFS, $D < h\nu$.[28]

Surprisingly, the shape of the spectrum of **1** is temperature-independent in the range 3−30 K; above 40 K the lines are increasingly broadened by spin relaxation processes, but appearance of other components is not observed. The invariance of the spectrum indicates a single distinct spin multiplet to give rise to the observed X-band resonances. This is somewhat unexpected since at elevated temperature the whole "spin ladder" of the coupled system is partially Boltzmann populated. According to the susceptibility result, $J_0 = -4.4$ cm^{-1}, the total exchange splitting of the spin states is only $\Delta = 52$ cm^{-1}

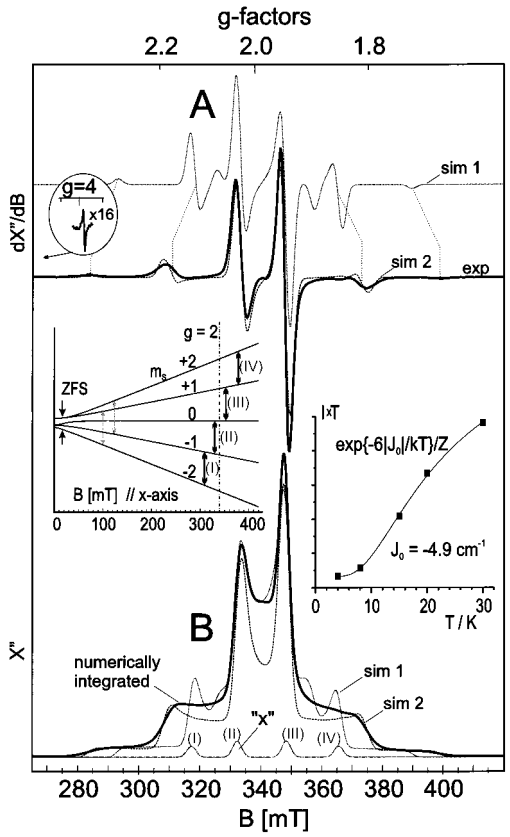

Figure 3. X-band EPR derivative spectrum (A) and integrated spectrum (B) of **1** in CH_3CN/DMF (1:3) solution and corresponding simulations. Experimental conditions: temperaure 30 K; microwave 9.450 GHz/1.6 mW; modulation 2 mT/100 kHz. Simulations for $S_t = 2$ by using eq 2 without fourth-order term (sim 1): $D_t = 0.0149$ cm^{-1}, $E/D_t = 0$, $g_t = 1.979$ (isotropic), Gaussian lines $W = 4$ mT (isotropic). Subspectrum ("x"): "single-crystal" type contribution to the simulated absorption spectrum (sim 1) for B parallel x. Simulations with fourth-order terms (sim 2): $D_t = 0.019$ cm^{-1}, $E/D_t = 0.02$, $B_4 = 1 \times 10^{-6}$ cm^{-1}, $B_4^0 = -5.9 \times 10^{-5}$ cm^{-1}, $g_t = 1.978$ (isotropic), Gaussian lines $W = 4.2$ mT (isotropic). Left inset: m_S-level scheme for B oriented in the x-direction with parameters as for sim 1. Right inset: Temperature dependence of the EPR intensities of **1** in CH_3CN/DMF (1:3) solution. The solid line is a fit with the Boltzmann function $I \times T =$ constant $\times$ $\exp\{-6|J_0|/kT\}/Z$ for the $S_t = 2$ manifold with $Z = [1 + 3\exp\{-2|J_0|/kT\} + 5\exp\{-6|J_0|/kT\}]$ being the corresponding partition function and $J_0 = -4.9$ cm^{-1} (ZFS neglected).

($=12|J_0|$), which corresponds to a temperature of 76 K ($= \Delta/k$). As expected, the intensity of the observed EPR spectrum exhibits a characteristic temperature dependence. Figure 3 (right inset) shows the values that are obtained in the range 4−30 K by double integration of the experimental derivative signals at "$g = 2$" measured under nonsaturating conditions. The variation of the temperature-weighted data (intensity $\times$ temperature vs temperature) is typical of excited-state resonances coming from a manifold well above an EPR-silent ground state. Systematic probing of the different multiplets of the spin-coupled system showed that the experimental result can be best reproduced with the Boltzmann function for the $S_t = 2$ quintet state. With the corresponding energy gap $\Delta E = 6|J_0|$ between $S_t = 2$ and the $S_t = 0$ ground state (see inset Figure 2) a value $J_0 = -4.9 \pm 0.5$ cm^{-1} is obtained for the exchange coupling constant. This is in convincing agreement with the result of the static magnetization measurement on solid material (−4.4 cm^{-1}). Corresponding simulations for the other manifolds yield either very unsatisfactory fits ($S_t = 1$) or inconsistent values for the exchange coupling constants ($S_t = 3$, $J_0 = -2$ cm^{-1}). Therefore the X-band EPR spectrum of **1** can be clearly assigned to the $S_t = 2$ state of the $Cr^{III}-Cr^{III}$ spin-coupled pair of the molecule, which is also corroborated by spin-Hamiltonian simulations given below. Hence, the EPR intensity data obtained from frozen solution and the magnetic susceptibility result for solid material are readily consistent and prove that the exchange interaction in complex **1** is *intramolecular*. It is mediated by the diamagnetic $Zn(dmg)_3$ "bridging ligand" between the terminal Cr^{III} ions. In contrast to this, the intermolecular interactions in the solid are negligibly small due to the merely through-space mechanism.

To conclude, we compare the strength of the exchange coupling prevailing in **1**, $Cr^{III}Zn^{II}Cr^{III}$, with that in the related isoelectronic **2**, $Mn^{IV}Zn^{II}Mn^{IV}$.[7,8] The Mn(IV) centers in **2** also exhibit antiparallel spin coupling, but the exchange interaction is remarkably stronger ($J = -19.2$ cm^{-1}),[7] although the Mn(IV)−Mn(IV) separation is ∼7 Å as well,[4] which is attributable to the higher charge on Mn(IV) than that on the Cr(III) center. Thus, the higher covalent character of the Mn(IV)−ligand bond leads to stronger electronic interactions.

Zero Field Splittings. The basic difference between the EPR properties of the $S_t = 2$ multiplet and the other coupled spin states of complex **1** owes its origin to different zero-field splittings of the multiplets. In the limiting case of dominating isotropic exchange interaction ($|J_0| \gg D_i$) for a symmetric dimer the ZFS parameters of each of the isolated integer-spin manifolds S_t can be derived from the local parameters (eq 1) by using a spin projection technique for $S_i = {}^3/_2$ which is an application of the Wigner−Eckart theorem:[27,31]

$$\tilde{\mathbf{D}}_1 = 2(-{}^6/_5)\tilde{\mathbf{D}}_i + {}^{17}/_{10}\tilde{\mathbf{j}} \quad (4a)$$

$$\tilde{\mathbf{D}}_2 = 0\tilde{\mathbf{D}}_i + {}^1/_2\tilde{\mathbf{j}} \quad (4b)$$

$$\tilde{\mathbf{D}}_3 = 2({}^1/_5)\tilde{\mathbf{D}}_i + {}^3/_{10}\tilde{\mathbf{j}} \quad (4c)$$

$\tilde{\mathbf{D}}_i$ is the diagonal matrix of the Cr^{III} single-ion ZFS with elements $D_{xx} = E_i - {}^1/_3D_i$, $D_{yy} = -E_i - {}^1/_3D_i$, $D_{zz} = {}^2/_3D_i$, $\tilde{\mathbf{D}}_1$, $\tilde{\mathbf{D}}_2$, and $\tilde{\mathbf{D}}_3$ are the corresponding ZFS tensors of the coupled states $S_t = 1$, 2, 3, and $\tilde{\mathbf{j}}$ is the traceless anisotropic coupling tensor. According to these relations (eqs 4) the quintet state $S_t = 2$ is distinguished, inasmuch as it has no single-ion contributions to its ZFS. Since in complex **1** the dipolar[27] and anisotropic exchange[32] interactions of the widely separated Cr(III) ions should be at least an order of magnitude smaller than the microwave quantum at X-band frequencies ($h\nu \approx 0.3$ cm^{-1}), EPR transitions are expected to occur for $S_t = 2$, whereas for $S_t = 1$ and $S_t = 3$ the local ZFS contributions can prevent EPR transitions if the Cr^{III} single-ion D_i and E_i values are large enough.

The X-band EPR spectrum of **1** could be simulated by using the effective spin-Hamiltonian (eq 2) for an isolated $S_t = 2$ multiplet. The approach appeared to be justified because the ZFS of Cr^{III} ions in octahedral coordination is usually less than 1 cm^{-1}, which is well below the strength of exchange coupling. However, when only the axial and rhombic ZFS parameters were used, the major part of the spectrum and the splittings of the outer lines cannot be well reproduced with the same set of parameters. In Figure 3 (trace sim 1) this is demonstrated for the derivative spectrum at "$g = 2$" and the respective absorption

(31) Scaringe, P. R.; Derek, J. H.; Hatfield, W. E. *Mol. Phys.* **1978**, *35*, 701.
(32) Owen, J.; Harris, E. A. In *Electron Paramagnetic Resonance*; Geschwind, S., Ed.; Plenum Press: New York, London, 1972; Chapter 6.

spectrum obtained by numerical integration. The m_S-level scheme according to this situation for a selected field orientation in the *x*-direction is depicted in Figure 3 (left inset), and the respective "single-crystal" subspectrum ("x") is shown in Figure 3B (bottom). The labels (I, ..., IV) at the EPR transitions in the level scheme indicate the order of lines in the "single-crystal" spectrum "x". A comparison of the line positions in "x" with the intensity distribution of the experimental powder spectrum suggests that the simulation (sim 1) could be improved if the outer lines (I and IV) for any spin packet "x" could be further moved out on the field axis, without affecting the inner lines. In the level scheme such a variation would correspond to an enhancement of the ZF shifts for the higher m_S levels (± 2), without affecting the lower m_S levels ($0,\pm 1$). (Without ZFS all allowed transitions (I...IV) would occur at the same resonance field at $g = 2$.) Since particularly such a modification of the usual ZFS scheme can be induced by ZFS terms of higher order in *S*, a symmetry-adapted fourth-order term was introduced in the effective spin Hamiltonian for $S_t = 2$ according to eq 3. With this extension, a very satisfactory simulation of the X-band spectrum was obtained (Figure 3, trace sim 2) with the parameter set $D_t = 0.019(2)$ cm^{-1}, $E/D_t = 0.02(3)$, $B_4 = 1(1) \times 10^{-6}$ cm^{-1}, $B_4^0 = -5.9(5) \times 10^{-5}$ cm^{-1}, $g_t = 1.978(1)$ isotropic. Similar good fits were obtained with these values for spectra measured at S- and Q-band frequencies (not shown here).

Zero-Field Splitting and Spin Coupling. It is unusual that EPR powder spectra have significant sensitivity for zero-field parameters of higher order than S^2. Correspondingly, such terms usually were not included in spin-Hamiltonian simulations of $S = 2$ powder spectra.[28,29,33] The question arose where such a term can originate from. Theoretically it *cannot* come from local Cr^{III} ligand-field and spin−orbit interactions because the low multiplicity of the local Cr^{III} spins $2S_i + 1 = 4$ is not sensitive to ZF interactions of higher degree. For this reason we alternatively investigated the influence of multiplet mixing by competing single-ion ZFS and exchange interaction in the coupled system. To this end the frozen solution spectra of **1** were simulated by using the full interaction matrix with the usual axial and rhombic S^2 terms for the local spins (eq 1). In the initial runs of the simulations all potential transitions within the coupled spin system were considered in the search and determination of resonances. For the subsequent parameter optimization only the transitions within the "$S_t = 2$" submanifold were used, since only this manifold is EPR active for the applied microwave frequencies (as expected from the considerations given above). For a systematic search in the spin Hamiltonian parameter space also frequency-dependent spectra were measured at Q- and S-band frequencies and analyzed together with the X-band data. Consistent and satisfactory fits were obtained in this program with identical parameters for all spectra, as shown in Figure 4. In the multifrequency simulations the value of the isotropic part of the exchange coupling was fixed to the value $J_0 = -4.4$ cm^{-1} determined from the static magnetic susceptibility measurement. The convincing fit of the simulations shows that the apparent ZFS of the spectra indeed can be readily explained by anisotropic spin coupling. The effect of this anisotropy cannot be replaced in the calculations by level mixing due to competition of isotropic exchange and *strong* Cr^{III} ZFS (>1 cm^{-1}). Completely different spectral patterns would be observed in this case. The best values for the anisotropic spin coupling tensor were found to be $\tilde{\mathbf{j}} = (0.0054(4), 0.0066(4), -0.012(2))$ cm^{-1}. Such a coupling strength can be easily explained by dipolar interaction[27,32] of the local Cr^{III} spins. Even in an oversimplified point-dipole model the spin−spin distance that could be deduced from $j_z = -0.012$ cm^{-1} is $d = 6.5$ Å, which is fairly close to the Cr···Cr nuclear distance in **1**. The small but significant rhombicity of the $\tilde{\mathbf{j}}$ tensor reveals deviation from axial symmetry for the spin density distribution in the compound. It results presumably from the "twist" of the basically trigonal coordination polyhedron of the Cr^{III} sites described above.

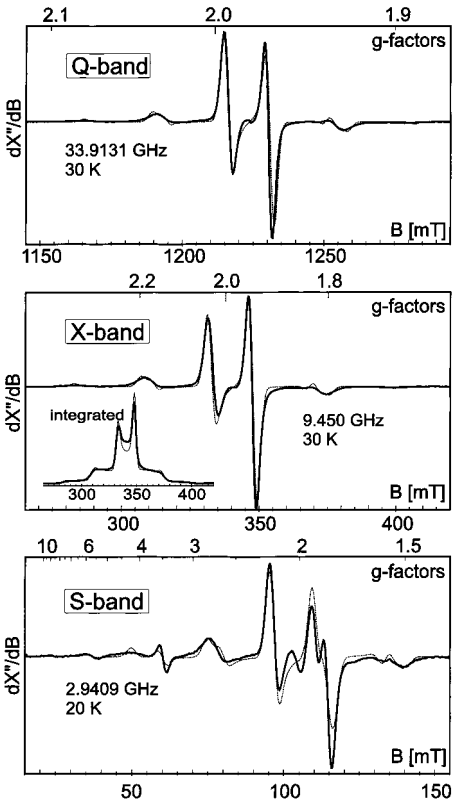

Figure 4. Q-, X-, and S-band EPR derivative spectra of **1** in CH_3CN/DMF (1:3) solution and spin-Hamiltonian simulations for the *coupled* system $S_i = 3/2$, $i = 1, 2$ according to eq 1. Experimental conditions, Q-band: temperaure 30 K; microwave 33.913 GHz/1 mW; modulation 0.4 mT/100 kHz. X-band: see Figure 3. S-band: temperaure 20 K; microwave 2.9409 GHz/1 mW; modulation 0.96 mT/100 kHz. Simulations with $D_i = 0.198$ cm^{-1}, $E/D_i = 0.102$, $g_i = 1.979$ (isotropic), $J_0 = -4.4$ cm^{-1}, $\tilde{\mathbf{j}} = (-0.0054, -0.0066, 0.012)$ cm^{-1}, Gaussian lines $W = 4$ mT (isotropic). The resolved splittings of the "sidebands" in the simulation (for instance at 310 mT and 375 mT at X-band) originate predominantly from the slight rhombicity of the $\tilde{\mathbf{j}}$ tensor. The broadening of these features and apparent absence of resolved splittings in the corresponding experimental traces is presumably due to inhomogeneous distribution of the $\tilde{\mathbf{j}}$ tensor components or the related ZFS, which is not included in the simulations. The X- and Q-band spectra show weak "forbidden" half-field transitions at $g \approx 4$ (not depicted here) which also could be satisfactorily simulated. The experimental X-band line at $g \approx 4$ is shown in Figure 3 (elliptical inset); at Q-band the corresponding line at 614 mT is about 5 times weaker.

The "higher order" effects in the above description of the EPR spectra of **1** by an effective Hamiltonian could be reproduced with the coupled Hamiltonian (eq 1) by sizable multiplet mixing due to the finite values for the Cr^{III} ZFS parameters. From fits of the experimental spectra the values $D_i = 0.198(2)$ cm^{-1} and $E/D_i = 0.102(50)$ were obtained for both Cr^{III} sites. They are well in the usual range reported for Cr^{III} compounds,[34−38] or other transition metal compounds with

(33) Barra, A. L.; Gatteschi, D.; Sessoli, R.; Abbati, G. L.; Cornia, A.; Fabretti, A. C.; Uytterhoeven, M. G. *Angew. Chem., Int. Ed. Engl.* **1997**, *36*, 2329.

(34) Singer, L. S. *J. Chem. Phys.* **1955**, *23*, 379.

electron configuration $(d_{xy})^1(d_{xz})^1(d_{yz})^1$ and spin $S = {}^3/_2$, like Mn^{IV},[39,40] V^{II},[41] and even Fe^V complexes.[42,43] We summarize that the multifrequency simulations for compound **1** allowed us to determine the ZFS of the local Cr^{III} ions from the $S_t = 2$ quintet state, which otherwise has no contributions from single-ion ZFS interactions. In this particular case, in contrast to what is observed for other integer-spin systems like mononuclear transition metal compounds or coupled systems with "high-spin" ground states,[33,44−47] the *lower* frequency S-band spectra show particularly high sensitivy for ZFS and the higher order effects.

Recently, quartic ZF terms have been introduced for the interpretation of low-temperature high-frequency EPR results,[45−47] data from inelastic-neutron-scattering and torque-magnetic susceptibility measurements[48] of single-molecule magnets. These materials[47,49−53] are transition metal compounds with Mn_{12}, Fe_8, Mn_4, Fe_4, or other polymetal ion cores and high total-spin ground states up to $S = 12$. It was pointed out that fourth-order spin terms are important for the understanding of the magnetic anisotropy of the materials and the rates of quantum tunneling of the magnetization. The B_n^m terms contribute to the mixing and the energy separation of the m_S states of the total spin multiplets and thus influence the height of the energy barrier for magnetization inversion and the pathway for resonance tunneling. Elaborate attempts were made to investigate the influence of multiplet mixing on the magnetic anisotropy in these systems, but the large spin multiplicities inhibit full-matrix descriptions of the spin−spin and ZF interactions. *With complex **1** we present a spin dimer which is not at all a single-molecule magnet but rather a simple example for which the origin of higher order spin terms could be experimentally studied and readily explained within the framework of a usual spin Hamiltonian description*. It is interesting to note that for instance the ZF- and exchange splittings of an "Fe_8" compound[54] with an $S = 10$ ground state[47,55] ($|D_{S=10}| \approx 0.2$ cm^{-1}, $[E_{S=10} - E_{S=9}] \approx 25$ cm^{-1}) are quite similar to corresponding splittings for **1** and it would be certainly interesting to unravel level mixing and single-ion anisotropy of the Fe^{III} sites ($S_i = {}^5/_2$).

Multiplet mixing or higher order spin terms have not been considered before in EPR investigations of isolated molecular Cr^{III} dimers.[27,56] Best described is the example of the strongly antiferromagnetically coupled tris(μ-hydroxo) bridged dimer[10] $[(tmtacn\ Cr^{III})_2(OH)_3]^{3+}$ ($J = -64$ cm^{-1}) for which the multiplet-dependent ZF parameters seems to obey the relations of eq 4.[38,57] Small deviations of temperature-dependent EPR spectra of $S_t = 1, 2, 3$ states from the properties predicted for a strongly coupled system have been attributed to temperature variations of the spin coupling constant due to magnetostriction effects. For compound **1** a sizable influence of magnetostriction was not observed. The effect which corresponds to a biquadratic contribution to the exchange[32] was described for susceptibility measurements of other Cr^{III} dimers.[58] In the single-crystal EPR work on Cr^{III} pairs prepared in spinel and inverse spinel host lattices,[59−61] biquadratic exchange (magnetostriction) and antisymmetric exchange[62,63] ($\mathbf{d}\cdot\boldsymbol{S}_1 \times \boldsymbol{S}_2$) was introduced to explain particularly the ZFS of the $S_t = 2$ excited-state manifold. Antisymmetric exchange, which occurs only for non-centrosymmetric spin systems, is interesting to study in single molecules, since it is responsible for the spin-canting of solid-state antiferromagnets and information about d values is still scarce for isolated systems. However, for the inverse spinel systems[61] multiplet mixing was neglected and it is reasonable to assume that the off-diagonal terms in the ZFS for the Cr^{III} pairs cause splittings of the $S_t = 2$ manifold comparable to those attributed to antisymmetric exchange. This fact was pointed out already by Münck et al.,[64] who reported evidence for antisymmetric exchange in an Fe^{III} dimer model compound with $d = 2.2$ cm^{-1}. For complex **1**, although being a non-centrosymmetric molecule, neither antisymmetric exchange nor biquadratic exchange terms play an important role for the interpretation of S-, X-, and Q-band EPR spectra in frozen solution and SQUID magnetometry of solid material.

Supporting Information Available: Tables of crystallographic information for compound **1**. This material is available free of charge via the Internet at http://pubs.acs.org.

Note Added after ASAP. The Supporting Information paragraph and link were omitted from the original version of this article published ASAP on Feb 10, 2001. The correct information is in the issue posted on Mar 5, 2001.

IC000870H

(35) McGarvey, B. R. *J. Chem. Phys.* **1964**, *41*, 3743.
(36) Pedersen, E.; Toftlund, H. *Inorg. Chem.* **1974**, *13*, 1603.
(37) Sommerville, D. A.; Jones, R. D.; Hoffmann, B. M.; Basolo, F. *J. Am. Chem. Soc.* **1977**, *99*, 8195.
(38) Bolster, D. E.; Gütlich, P.; Hatfield, W. E.; Kremer, S.; Müller, E. W.; Wieghardt, K. *Inorg. Chem.* **1983**, *22*, 1725.
(39) Camenzind, M. J.; Hollander, F. J.; Hill, C. L. *Inorg. Chem.* **1983**, *22*, 3776.
(40) Duboc-Toia, C.; Hummel., H.; Bill, E., Barra A.-L.; Chouteau, G.; Wieghardt, K. *Angew. Chem.*, in press
(41) Jacobsen, C. J. H.; Pedersen, E.; Villadsen, J.; Weihe, H. *Inorg. Chem.* **1993**, *32*, 1216.
(42) Meyer, K.; Bill, E.; Mienert, B.; Weyhermüller, T.; Wieghardt, K. *J. Am. Chem. Soc.* **1999**, *121*, 4859.
(43) Grapperhaus, C. A.; Mienert, B.; Bill, E.; Weyhermüller, T.; Wieghardt, K. *Inorg. Chem.* **2000**, *39*, 5306.
(44) Aubin, S. M. J.; Dilley, N. R.; Pardi, L.; Krystek, J.; Wemple, M. W.; Brunel, L.-C.; Maple, M. B.; Christou, G.; Hendrickson, D. N. *J. Am. Chem. Soc.* **1998**, *120*, 4991−5004.
(45) Barra, A. L.; Gatteschi, D.; Sessoli, R. *Phys. Rev. B* **1997**, *56*, 8192−8198.
(46) Barra, A. L.; Caneschi, A.; Gatteschi, D.; Sessoli, R. *J. Magn. Magn. Mater.* **1998**, *177*, 709−710.
(47) Barra, A. L.; Gatteschi, D.; Sessoli, R. *Chem.—Eur. J.* **2000**, *6*, 1608−1614.
(48) Cornia, A.; Affronte, M.; Jansen, A. G. M.; Gatteschi, D.; Caneschi, A.; Sessoli, R. *Chem. Phys. Lett.* **2000**, *322*, 477−482.
(49) Sun, Z. M.; Grant, C. M.; Castro, S. L.; Hendrickson, D. N.; Christou, G. *Chem. Commun.* **1998**, 721−722.
(50) Castro, S. L.; Sun, Z. M.; Grant, C. M.; Bollinger, J. C.; Hendrickson, D. N.; Christou, G. *J. Am. Chem. Soc.* **1998**, *120*, 2365−2375.
(51) Clemente-Leon, M.; Soyer, H.; Coronando, E.; Mingotaud, C.; Gomez-Garcia, C. J.; Delhaes, P. *Angew. Chem., Int. Ed.* **1998**, *37*, 2842−2845.
(52) Brechin, E. K.; Yoo, J.; Nakano, M.; Huffman, J. C.; Hendrickson, D. N.; Christou, G. *Chem. Commun.* **1999**, 783−784.
(53) Barra, A. L.; Caneschi, A.; Cornia, A.; de Biani, F. F.; Gatteschi, D.; Sangregorio, C.; Sessoli, R.; Sorace, L. *J. Am. Chem. Soc.* **1999**, *121*, 5302−5310.
(54) Wieghardt, K.; Pohl, K.; Jibril, I.; Huttner, G. *Angew. Chem., Int. Ed. Engl.* **1984**, *23*, 77−78.
(55) Barra, A. L.; Debrunner, P.; Gatteschi, D.; Schulz, C. E.; Sessoli, R. *Europhys. Lett.* **1996**, *35*, 133−138.
(56) Glerup, J.; Hodgson, D. J.; Pedersen, D. *Acta Chem. Scand., Ser. A* **1983**, *A37*, 161.
(57) Kremer, S. *Inorg. Chem.* **1985**, *24*, 887−890.
(58) Hodgson, D. *Prog. Inorg. Chem.* **1975**, *19*, 186.
(59) Henning, J. C. M.; Boom, H. v. d. *Phys. Rev. B* **1973**, *8*, 2255−2262.
(60) Henning, J. C. M.; Boef, J. H. d.; Gorkom, G. P. v. *Phys. Rev. B* **1973**, *7*, 1825−1833.
(61) Gutowski, M. *Phys. Rev. B* **1978**, *18*, 5984−5989.
(62) Moriya, T. In *Magnetism*; Rado, G. T., Suhl, H., Eds.; Academic Press Inc.: New York and London, 1963; Vol. I, pp 86−124.
(63) Dzyaloshinsky, I. *J. Phys. Chem. Solids* **1958**, *4*, 241−255.
(64) Kauffmann, K. E.; Popescu, C. V.; Dong, Y.; Lipscomb, J. D.; Que, L.; Münck, E. *J. Am. Chem. Soc.* **1998**, *120*, 8739−8746.